Chaos, Solitons & Fractals 59 (2014) 13–27

Contents lists available at ScienceDirect

Chaos, Solitons & Fractals

Nonlinear Science, and Nonequilibrium and Complex Phenomena

journal homepage: www.elsevier.com/locate/chaos

Superstable credit cycles and U-sequence

Iryna Sushko [a,b,*], Laura Gardini [c], Kiminori Matsuyama [d]

[a] Institute of Mathematics NASU, 3 Tereshchenkivska str., 01601 Kyiv, Ukraine
[b] Kyiv School of Economics, Yakira str. 13, 04119 Kyiv, Ukraine
[c] Department of Economics, Society and Politics, University of Urbino, Via Saffi 42, 61029 Urbino, Italy
[d] Department of Economics, Northwestern University, 2001 Sheridan Road, Evanston, IL 60208, USA

ARTICLE INFO

Article history:
Received 26 July 2013
Accepted 16 November 2013

ABSTRACT

We study a particular bifurcation structure observed in the parameter space of a one-dimensional continuous piecewise smooth map generated by the credit cycle model introduced by Matsuyama, where the map is defined over the absorbing interval via three functions, one of which is a constant. We show that the flat branch gives rise to superstable cycles whose periodicity regions are ordered according to a modified U-sequence and accumulate to the curves related to homoclinic cycles which represent attractors in Milnor sense. The boundaries of these regions correspond to fold and flip border collision bifurcations of the related superstable cycles.

© 2013 Elsevier Ltd. All rights reserved.

1. Introduction

Piecewise smooth dynamical systems have recently become quite a popular topic of research. Such an increasing interest towards nonsmooth dynamics comes both from purely theoretical problems and from various applied fields of science. In fact, particular real processes characterized by "nonsmooth" phenomena (such as sharp switching, impacts, friction, sliding and the like), are quite often modeled by means of piecewise smooth functions, continuous or discontinuous. Among numerous examples the most known are switching electronic circuits, such as DC–DC converters, mechanical systems with impacts or stick–slip motion, relay control systems, etc. (for the related references and further examples from electronics, mechanics, control and other fields see [8,5,36,14]). Nonsmooth dynamical systems appear naturally also in economics and other social sciences when, for instance, some decision-making process is modeled using logic functions, or if an optimization problem is solved taking into account limited resources or non-negativity constrains, and so forth. For example, several oligopoly models with different kinds of constraints are considered in [32,6]. It is worth to mention also the papers dealing with nonsmooth maps related to economic and financial market modeling (see [12,18,23,16,19,35], to cite a few).

General theory of dynamical systems generated by nonsmooth functions has not yet such a complete form as the one established for smooth systems. As an important advancement towards such a theory for piecewise smooth continuous-time systems (flows) one has to mention [14] where so-called *discontinuity-induced bifurcations* are classified by means of properly constructed Poincaré maps (see also [29,11]). A classification of bifurcations in piecewise smooth maps is also proposed. An overview of different bifurcation scenarios observed in nonsmooth flows can be found in [36] (see also [37]) illustrated by applications from mechanical engineering, electronics and economics. It is worth to mention also earlier works, such as [26], in which bifurcation structures in nonsmooth continuous and discontinuous one-dimensional (1D for short) maps are investigated, as well as [15] (see also [13]) in which bifurcations occurring in nonsmooth n-dimensional continuous systems (called C-bifurcations) are classified.

The map considered in the present paper arises from an economic application. Namely, we investigate dynamics of the credit cycle model which is a particular case of the

* Corresponding author at: Institute of Mathematics NASU, 3 Tereshchenkivska str., 01601 Kyiv, Ukraine.
E-mail addresses: sushko@imath.kiev.ua (I. Sushko), laura.gardini@uniurb.it (L. Gardini), k-matsuyama@northwestern.edu (K. Matsuyama).

0960-0779/$ - see front matter © 2013 Elsevier Ltd. All rights reserved.
http://dx.doi.org/10.1016/j.chaos.2013.11.006

more generic model of credit cycles introduced in [22] (see also [24]). It is described by a 1D continuous piecewise smooth map depending on four parameters and defined by three smooth functions among which one is a constant. This map possesses quite a rich dynamic behavior, and we are interested in understanding how the particular bifurcation structure, observed in its parameter space, is organized. By *bifurcation structure* we mean the partition of the parameter space of a map into regions related to qualitatively similar asymptotic dynamics. Clearly, the boundaries of such regions are defined by the parameter values corresponding to certain bifurcations. In fact, one of the characteristic features of nonsmooth dynamics is the occurrence of so-called *border collision bifurcation* (BCB for short), see [30,31,4]. Recall that the BCB occurs when, under variation of some parameters, an invariant set (for example, a fixed point or a cycle) collides with a border at which the system changes the function in its definition, and this collision leads to a qualitative change in the dynamics. Such a change can be quite drastic: for example, one can observe the transition from an attracting fixed point to an attracting cycle of any period, or directly to a chaotic attractor, that is impossible in smooth dynamical systems. Thus, the bifurcation structure of the parameter space of a piecewise smooth map may be defined, besides standard "smooth" bifurcations, by the BCBs as well. The possible results of a generic BCB of an attracting cycle of a 1D continuous piecewise smooth map with one border point can be rigorously classified depending on the parameters using *1D BCB normal form*, which is the well known skew tent map defined by two linear functions. The dynamics of the skew tent map are completely described depending on the slopes of the linear branches (see [20,21]), that makes it possible to use this map as a BCB normal form (see [30,31,33]).

Besides nonsmoothness, another notable feature of the considered map is, as already mentioned, the presence in its definition of a flat branch. Obviously, for a piecewise smooth map with a flat branch any cycle with a point on that branch is *superstable*, moreover, any initial condition from its basin of attraction is *preperiodic* to such a cycle, that means it is mapped into the cycle in a *finite* number of iterations, namely, as soon as the trajectory reaches the flat branch. From an applied point of view it may be important that superstable cycles related to a flat branch, differently from "smooth" superstable cycles, are persistent under parameter perturbations. That is, in the parameter space there are open regions related to these cycles. Clearly, the boundaries of such periodicity regions can be defined only by BCBs of the related cycles given that the zero eigenvalue does not allow any other bifurcation.

The overall bifurcation structure of the parameter space of a piecewise smooth map with a flat branch obviously depends on the particular map (see [9,7,2]). Our aim is to show that in the parameter space of the considered map the periodicity regions of superstable cycles are organized according to the well known *U-sequence* (first described in [27], see also [9,17]) which is characteristic for unimodal maps. It consists of two-letter symbolic sequences ordered for monotonically increasing/decreasing parameter value according to the appearance of the related cycles. We adjust the U-sequence to the considered map by introducing one more letter related to the flat branch, that does not influence the basic rule of formation of the U-sequence. However, it is important to emphasize that in the U-sequence of our map the *harmonics* are related to infinite cascades of *flip BCBs* (not of standard flip, or period-doubling, bifurcations), and that the first symbolic sequence in any of such a cascade is related to the cycle born due to *fold BCB* (not to standard fold, or tangent, bifurcation).

Considering the overall bifurcation structure in two different parameter planes, we notice that the periodicity regions, ordered in the U-sequence, are accumulating to particular curves. It is natural to suppose that such curves are related to the *homoclinic bifurcations* of the corresponding unstable cycles (cf. with the parameter values of the logistic map related to the homoclinic bifurcations of its unstable cycles, to which periodic windows are accumulating). However, a homoclinic cycle (i.e., the cycle at the moment of its homoclinic bifurcation) of the considered map, being locally unstable, is an attractor in Milnor sense because a positive measure set of initial points of the absorbing interval is mapped into this cycle (see [3] for the discussion of similar attractors in a discontinuous map). That differs from a homoclinic cycle of the logistic map into which only a zero-measure set of initial points (formed by all the preimages of the cycle and called stable set) is mapped.

The plan of the work is as follows. In the next section we first define the map and explain meaning of its main variable and parameters from economic point of view. Then we obtain stability conditions of the fixed points, specify the region in the parameter space corresponding to the case in which the map is defined over the absorbing interval via all the three functions, introduce the symbolic sequences for the superstable cycles and define their basin of attraction. In Section 3 we present some numerical results, namely, the 1D and 2D bifurcation diagrams which illustrate the bifurcation structures formed by the periodicity regions related to the superstable cycles. We show that the boundaries of these regions correspond to the fold and flip BCBs, as well as persistence border collisions. Then we present the curves related to the first homoclinic bifurcations of the fixed point and of the 2-cycle, obtained using the conditions of these bifurcations. Examples of homoclinic cycles and their stable sets are also discussed. In Section 4 we recall some basic rules of the formation of the standard U-sequence, and then adjust it to the considered map. In such a way we get the order in which the periodicity regions of the superstable cycles are organized. Section 5 concludes.

2. Description of the map. Preliminaries

We consider a 4-parameter family of 1D piecewise smooth maps $f:[0,1]\to[0,1]$ defined as follows:

$$f: x \mapsto f(x) = \begin{cases} x^{\alpha} & \text{for } 0 \leqslant x \leqslant x_c, \\ \left[\max\left\{\frac{1}{\mu\beta}\left(1-\frac{x}{m}\right), \frac{1}{\beta}\right\}\right]^{\frac{\alpha}{1-\alpha}} & \text{for } x > x_c, \end{cases} \tag{1}$$

where α, β, μ and m are real parameters such that

$$0 < \alpha, \mu < 1, \quad \beta \equiv B\frac{1-\alpha}{\alpha} > 0, \quad 1 < m < \frac{1}{1-\alpha} \tag{2}$$

and x_c is the *border point* defined by

$$x_c^{1-\alpha} = \frac{1}{\mu\beta}\max\left\{1 - \frac{x_c}{m}, \mu\right\}. \tag{3}$$

Depending on the parameters, the map f can be defined by at most three branches (see Fig. 1) which we denote as follows:

- $f_L(x) \equiv x^\alpha$ (the monotone increasing branch);
- $f_M(x) \equiv \left[\frac{1}{\mu\beta}\left(1 - \frac{x}{m}\right)\right]^{\frac{\alpha}{1-\alpha}}$ (the monotone decreasing branch);
- $f_R(x) \equiv \left(\frac{1}{\beta}\right)^{\frac{\alpha}{1-\alpha}} \equiv \widehat{x}$ (the flat branch).

The border point x_c can be defined either from $f_L(x_c) = f_M(x_c)$, in which case we denote it as x_l:

$$x_c \equiv x_l: \quad x_l^{1-\alpha} = \left[\frac{1}{\mu\beta}\left(1 - \frac{x_l}{m}\right)\right] \tag{4}$$

or from $f_L(x_c) = f_R(x_c)$, in which case we get

$$x_c \equiv x_m = \left(\widehat{x}\right)^{\frac{1}{\alpha}} = \left(\frac{1}{\beta}\right)^{\frac{1}{1-\alpha}}. \tag{5}$$

One more possible border point, denoted x_r, is related to the max function and obtained from $f_M(x_r) = f_R(x_r)$, so that:

$$x_r = m(1-\mu). \tag{6}$$

Before investigating the dynamic properties of the map f let us explain meaning of the variable x and parameters α, β, μ and m from economic point of view, and clarify briefly why the map f has three (upward-sloping, downsloping, and constant) branches.

The map describes the dynamic trajectory of the entrepreneur *net worth* x in a credit cycle model, first introduced in [22], under the additional assumption that the aggregate production function is Cobb–Douglas, see [25]. In this model, generations of entrepreneurs arrive sequentially. When they arrive, they first sell their labor and other inputs to the production of the consumption good to acquire some net worth, which they could later use to finance their own projects or lend to finance the projects run by others. There are two types of projects, *the Good* and *the Bad*. The Good projects produce capital, which contributes to the production, together with labor and other inputs supplied by others who could undertake projects in the future. By competing for these inputs, more Good projects drive up the prices of these inputs, thereby improving the net worth of next generations of entrepreneurs who supply these inputs. This also means that they are subject to diminishing returns. In contrast, the Bad projects are independently profitable as they directly produce the consumption good. In other words, they do not require the inputs supplied by others. This means that they fail to improve the net worth of next generations of entrepreneurs, and that they are not subject to diminishing returns. However, they are subject to borrowing constraints because their revenues are not fully pledgeable, which means that the entrepreneurs need to have some net worth of their own to finance them. One can show that, in this setting, the equilibrium composition of the credit flows between the Good and the Bad depends on the current net worth, as follows:

- When the current net worth x is low ($x < x_l$), the entrepreneurs cannot finance the Bad projects, because the borrowing constraint is too tight. All credit thus flows into the Good projects, even after the rate of return of the Good projects become lower than that of the Bad projects, and hence, a higher current net worth leads to a higher net worth in the next period. This explains the *upward-sloping branch* $f_L(x)$.

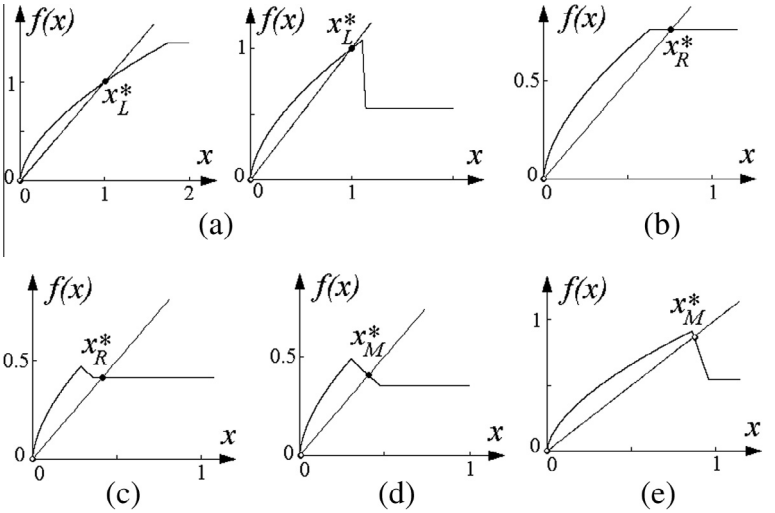

Fig. 1. The map f and its fixed points at $\mu = 0.4$, $\beta = 0.8$ in (a) on the left, and $\mu = 0.05$, $\beta = 1.5$ in (a) on the right (these parameter values belong to the region *A*, see Fig. 2); (b) $\mu = 0.7$, $\beta = 1.2$ (the region *B*); (c) $\mu = 0.7$, $\beta = 1.8$ (the region *C*); (d) $\mu = 0.6$, $\beta = 2$ (the region *D*); (e) $\mu = 0.2$, $\beta = 1.5$ (the region *E-I*). The other parameter values are $m = 1.2$ and $\alpha = 0.6$.

- When the current net worth is in the intermediate range, $(x_l < x < x_r)$, the Bad projects are financed but still subject to the borrowing constraint, so that the rate of return of the Bad projects remain strictly higher than that of the Good projects. Thus, a higher current net worth, by easing the borrowing constraint of the Bad projects, thereby making them more appealing to the lenders, reduces the credit flow to the Good, which causes a net worth decline in the next period. This explains the *downward-sloping branch* $f_M(x)$.
- When the current net worth is high $(x > x_r)$, the Bad projects are no longer subject to the borrowing constraint, so that both Good and Bad projects earn the same rate of return in equilibrium. With the Good being subject to diminishing returns, all additional credit flow into the Bad, not at all to the Good, hence the net worth in the next period, is independent of the current net worth. This explains the *constant branch* $f_R(x)$.

Meaning of the model parameters is the following:

- α represents the share of capital in the Cobb–Douglas production function, which determines how strongly the Good projects are subject to diminishing returns;
- B represents the (constant) rate of return of the Bad projects;
- μ represents the pledgeability of the Bad projects (thus, $\mu = 1$ is the fully pledgeable case, where the borrowing constraint is never binding, while $\mu = 0$ is no pledgeable case, so that the entrepreneurs cannot borrow at all to finance the Bad projects, so that they must rely entirely on their own net worth);
- m represents the fixed investment size of the Bad projects.

For more detailed discussion of the general case see [22,24], and for the Cobb–Douglas case see [25].

Now let us summarize some simple properties of the map f and specify the parameter region we are interested in.

In the simplest case, defined by the condition $x_m \geqslant x_r$, that holds for $\beta \leqslant (m(1-\mu))^{\alpha-1}$, the map f is given by the branches $f_L(x)$ and $f_R(x)$ only. The boundary in the parameter space denoted BC and defined as

$$BC: \qquad \beta = (m(1-\mu))^{\alpha-1} \tag{7}$$

is related to the appearance of the middle branch in the definition of f. Namely, for $\beta > (m(1-\mu))^{\alpha-1}$ the map f can be written in the following form:

$$f: x \mapsto f(x) = \begin{cases} f_L(x) = x^\alpha & \text{for } 0 \leqslant x \leqslant x_l, \\ f_M(x) = \left[\frac{1}{\mu\beta}\left(1-\frac{x}{m}\right)\right]^{\frac{\alpha}{1-\alpha}} & \text{for } x_l < x \leqslant x_r, \\ f_R(x) = \widehat{x} & \text{for } x > x_r. \end{cases} \tag{8}$$

It is easy to see that besides the unstable fixed point in the origin the map f has one more fixed point denoted $x_i^*,\ i \in \{L, M, R\}$, which can be associated with any one of the functions $f_i(x)$. Existence and stability properties of x_i^* are discussed below and illustrated in Figs. 1 and 2.

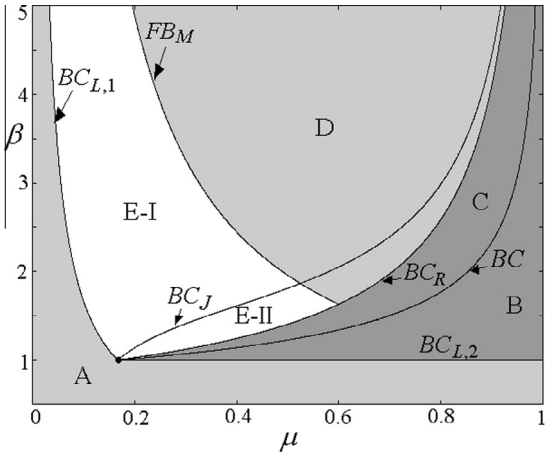

Fig. 2. Partition of the (μ, β)-parameter plane at $m = 1.2,\ \alpha = 0.6$. The region A corresponds to the stable fixed point x_L^*; $B \cup C$ to the superstable fixed point x_R^*; D to the stable fixed point x_M^*; *E-I* is related to the map f defined over the absorbing interval $J = [f^2(x_l), f(x_l)]$ by $f_L(x)$ and $f_M(x)$, and for *E-II* in the absorbing interval $J = [f(x_r), f(x_l)]$ the flat branch $f_R(x)$ is defined as well.

The nonzero fixed point related to $f_L(x)$ is given by $x_L^* = 1$ (see Fig. 1(a)). It exists for the parameter values belonging to the region denoted A and defined by

$$A: \qquad \beta \leqslant \max\left\{\frac{1}{\mu}\left(1-\frac{1}{m}\right), 1\right\} \tag{9}$$

(see Fig. 2). The two boundaries of A correspond to the BCBs of x_L^* at which $x_L^* = x_c$, namely, if the parameter point belongs to the boundary

$$BC_{L,1}: \qquad \beta = \frac{1}{\mu}\left(1-\frac{1}{m}\right), \tag{10}$$

we have $x_L^* = x_l$, and for

$$BC_{L,2}: \qquad \beta = 1, \tag{11}$$

we have $x_L^* = x_m$. If x_L^* exists, it is globally attracting. Note that in such a case we have $x_c \geqslant 1$, so that the map f in the interval $I = [0, 1]$ is defined by the branch $f_L(x)$ only.

The fixed point denoted x_R^* is related to the flat branch $f_R(x)$ and given by $x_R^* = \widehat{x}$. Clearly, $x_R^* < 1$, and x_R^* exists if $\widehat{x} \geqslant x_m$ (as in Fig. 1(b)) or if $\widehat{x} \geqslant x_r$ (as in Fig. 1(c)) that holds for the parameter region defined by

$$1 < \beta < (m(1-\mu))^{1-\frac{1}{\alpha}}. \tag{12}$$

If x_R^* exists, it is a superstable fixed point, globally attracting. At the boundary $\beta = 1$ (denoted as $BC_{L,2}$ in (11)) $x_R^* = x_m$, moreover, $x_R^* = x_L^* = 1$. If the parameter point crosses $BC_{L,2}$ we observe the transition from the superstable fixed point x_R^* to the stable fixed point x_L^* (for example, see the transition from Fig. 1(b) to Fig. 1(a) on the left), so that it is the so-called *persistence border collision*.[1] While at the boundary

$$BC_R: \qquad \beta = (m(1-\mu))^{1-\frac{1}{\alpha}}, \tag{13}$$

[1] Recall that *persistence border collision* of a fixed point occurs when the fixed point crosses the border without changing stability.

we have $x_R^* = x_r$, so that BC_R is related to one more border collision of x_R^*. The region of existence of x_R^* is divided by the boundary BC given in (7) in two subregions, denoted B and C:

$$B: \quad 1 < \beta < (m(1-\mu))^{\alpha-1}, \tag{14}$$

$$C: \quad (m(1-\mu))^{\alpha-1} < \beta < (m(1-\mu))^{1-\frac{1}{\alpha}} \tag{15}$$

(see Fig. 2).

Finally, the fixed point x_M^* of the map f related to the middle branch $f_M(x)$ is implicitly defined by $x_M^* = \left[\frac{1}{\mu\beta}\left(1-\frac{x_M^*}{m}\right)\right]^{\frac{\alpha}{1-\alpha}}$ (see Fig. 1(d) and (e)). It exists if $x_l \leqslant x_M^* \leqslant x_r$, and this is satisfied for parameter values belonging to the region defined by

$$\beta \geqslant \max\left\{\frac{1}{\mu}\left(1-\frac{1}{m}\right), (m(1-\mu))^{1-\frac{1}{\alpha}}\right\}. \tag{16}$$

Both boundaries of this region are related to the border collision of x_M^*, namely, at the boundary $BC_{L,1}$ (see (10)) we have $x_M^* = x_l$, moreover, $x_M^* = x_L^* = 1$, so that if the parameter point crosses $BC_{L,1}$ we observe the transition from the fixed point x_M^* to the stable fixed point x_L^* (for example, see the transition from Fig. 1(e) to Fig. 1(a) on the right). While at the boundary BC_R (see (13)) we have $x_M^* = x_r$, moreover, $x_M^* = x_R^*$ so that crossing BC_R we observe the transition from the superstable fixed point x_R^* to the fixed point x_M^* (see, for example, the transition from Fig. 1(d) to Fig. 1(c)). The slope of $f_M(x)$ at the fixed point x_M^* is negative, so that this fixed point may become unstable via a flip bifurcation (which is subcritical for $\alpha < 0.5$, degenerate [34] for $\alpha = 0.5$ and supercritical for $\alpha > 0.5$). The flip bifurcation curve of x_M^* is given by

$$FB_M: \quad \beta = \frac{\alpha}{\mu}(m(1-\alpha))^{1-\frac{1}{\alpha}}. \tag{17}$$

Thus, for parameter values belonging to the region denoted D defined by

$$D: \quad \beta > \max\left\{\frac{\alpha}{\mu}(m(1-\alpha))^{1-\frac{1}{\alpha}}, (m(1-\mu))^{1-\frac{1}{\alpha}}\right\}$$

(see Fig. 2) there exists the locally attracting fixed point x_M^*.

Let us define now an *invariant absorbing interval* of the map f given in (8), denoted J. There are two possibilities:

(1) In the absorbing interval J only the functions $f_L(x)$ and $f_M(x)$ are defined, that holds for parameter values belonging to the region denoted *E-I* and defined as

$$E\text{-}I: \begin{cases} \beta < \frac{\alpha}{\mu}(m(1-\alpha))^{1-\frac{1}{\alpha}}, \\ \beta > \max\left\{\frac{1}{\mu}\left(1-\frac{1}{m}\right),\ 1-\frac{1}{\mu}+\frac{1}{\mu}(m(1-\mu))^{1-\frac{1}{\alpha}}\right\} \end{cases} \tag{18}$$

(see Fig. 2). In such a case $J = [f^2(x_l), f(x_l)]$ (an example is shown in Fig. 3(a)).

(2) All the three functions, $f_L(x)$, $f_M(x)$ and $f_R(x)$, are involved in J, that holds in the region denoted *E-II* and given by

$$E\text{-}II: \begin{cases} \beta > (m(1-\mu))^{1-\frac{1}{\alpha}}, \\ \beta < \min\left\{1-\frac{1}{\mu}+\frac{1}{\mu}(m(1-\mu))^{1-\frac{1}{\alpha}}, \frac{\alpha}{\mu}(m(1-\alpha))^{1-\frac{1}{\alpha}}\right\} \end{cases} \tag{19}$$

(see Fig. 2). In such a case $J = [f(x_r), f(x_l)] = [\widehat{x}, f(x_l)]$ (see Fig. 3(b) for an example). The contact of J with the border point x_r, occurring when the condition $f(x_l) = x_r$ is satisfied, corresponds to the boundary

$$BC_J: \quad \beta = 1 - \frac{1}{\mu} + \frac{1}{\mu}(m(1-\mu))^{1-\frac{1}{\alpha}}. \tag{20}$$

All the parameter regions and bifurcation curves introduced above are illustrated in Fig. 2. As an economic interpretation of this figure we notice, in particular, that the unique fixed point x_M^* is unstable (*E-I* or *E-II*) or oscillatory stable (*D*), if the Bad projects are highly profitable (a high B, and hence a high β) and the pledgeability of their revenues (μ) is in the intermediate range (if it were sufficiently close to one, the entrepreneurs could finance them even with a low net worth, and if it is sufficiently close to zero, the entrepreneurs could not finance them even with a high net worth).

Preliminary description of the bifurcation structure of the region *E-I* is discussed in [25]. The main object of the present paper is the bifurcation structure of the region *E-II*, formed by the periodicity regions related to superstable cycles of the map f existing due to its flat branch. From now on we shall consider the parameter values belonging to the region *E-II*.

To distinguish between different cycles with the same period it is quite convenient to use their symbolic representation. To write down the *symbolic sequence* of an n-cycle $\gamma_n = \{x_i\}_{i=1}^n$ of the map f given in (8) we need at most 5 symbols: the symbol L is used for the periodic points $x_i : 0 < x_i < x_l$, the symbol M is reserved for $x_i : x_l < x_i < x_r$, the symbol R is used for $x_i : x_i > x_r$, and the symbols C_l and C_r are used for $x_i = x_l$ and $x_i = x_r$, respectively. In such a way the symbolic sequence, denoted σ, of the cycle γ_n consists of n symbols related to the location of the periodic points: $\sigma = \sigma_1\sigma_2\ldots\sigma_n, \sigma_i \in \{L, C_l, M, C_r, R\}$.

Let γ_n be a superstable cycle of the map f, and let $x_1 > x_r$, so that the first symbol of the symbolic sequence of γ_n is R (given that any cycle can have at most one point in the definition region of $f_R(x)$, the symbolic sequence of such a cycle has only one symbol R). Then $x_2 = f_R(x_1) = \widehat{x}$, that is, any superstable cycle of the map f consists of the point $\widehat{x}$ and its $n-1$ images by f. Obviously, two superstable cycles cannot coexist, while coexistence of a superstable cycle and a stable cycle (with symbolic sequence consisting of symbols L and M only) is possible, as well as coexistence of stable fixed point and stable 2-cycle.

The *basin of attraction* of any superstable cycle γ_n denoted $\mathcal{S}$ is given by the interval $[x_r, \infty)$ related to the flat branch, and the preimages of any rank $i > 0$ of the interval $[x_r, f_L(x_l)]$:

$$\mathcal{S} = \cup_{i=1}^{\infty} f^{-i}([x_r, f_L(x_l)]) \cup [x_r, \infty). \tag{21}$$

Obviously, any point of $\mathcal{S}$ is preperiodic to γ_n, that is, it is mapped into γ_n in a finite number of iterations. Note that due to noninvertibility of f, its inverse function is not uniquely defined, so that constructing the set $\mathcal{S}$ one has to include all the preimages of the interval $[x_r, f_L(x_l)]$ by all the three branches of the inverse function. See, for example, Fig. 4 which shows the map f, its superstable 3-cycle

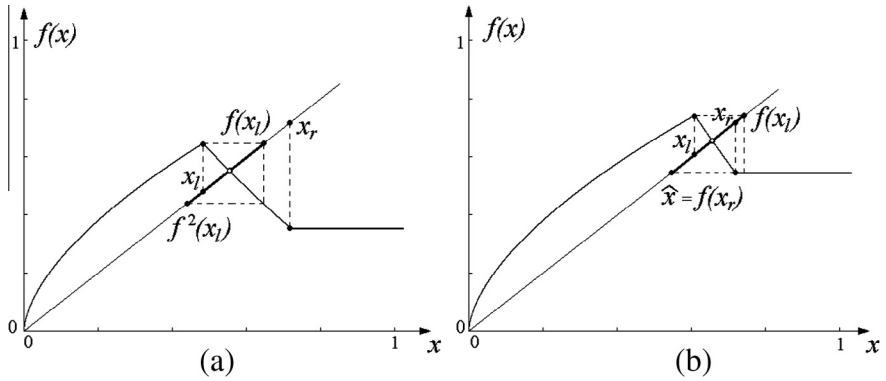

Fig. 3. The invariant absorbing interval $J = [f^2(x_l), f(x_l)]$ in (a) and $J = [f(x_r), f(x_l)]$ in (b) of the map f for the parameter values belonging to the regions *E-I* and *E-II*, respectively. Here $m = 1.2$, $\alpha = 0.6$, $\mu = 0.4$ and $\beta = 2$ in (a), $\beta = 1.5$ in (b).

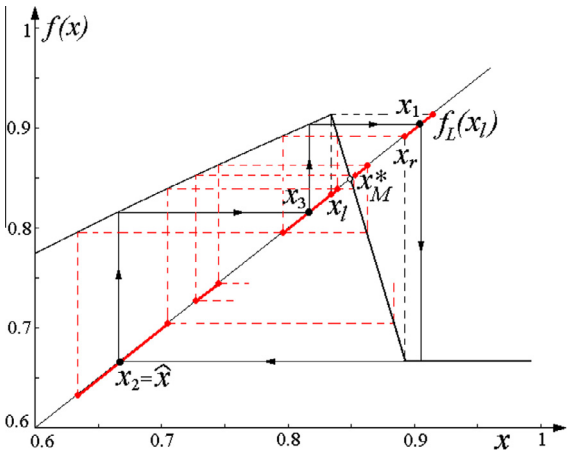

Fig. 4. The map f and its superstable cycle $\gamma_3 = \{x_i\}_{i=1}^3$. Basin of attraction of γ_3 includes the interval $[x_r, f_L(x_l)]$ and all its preimages (several of them are shown by thick lines). Here $m = 1.05$, $B = 1.5$, $\alpha = 0.5$ and $\mu = 0.15$.

$\gamma_3 = \{f_L^2(\hat{x}), \hat{x}, f_L(\hat{x})\}$ with the symbolic sequence RL^2, and the interval $[x_r, f_L(x_l)]$ together with a few its preimages. In this case the set of preimages of any rank fills densely the absorbing interval $J = [\hat{x}, f(x_l)]$. However, it is clear that not all the points of J are mapped into γ_3. There exists an invariant set of points which are not mapped into the cycle γ_3, defining its basin boundary, which is a chaotic repeller (of zero Lebesgue measure) consisting of the points of all the repelling cycles, their preimages of any rank and an uncountable set of aperiodic orbits. Indeed, it can be shown that for any superstable cycle γ_n its basin boundary has such a complicated structure, except for the superstable 2-cycle and its harmonics (that is, the 2^k-cycles, $k > 1$, born due to a cascade of flip BCBs of the 2-cycle) as we clarify in next sections.

3. Numerical results

In this section we present numerical results illustrating the bifurcation structure of the region *E-II* in the parameter space of the map f, related to its *superstable cycles*.

The 2D bifurcation diagram in the (μ, β)-parameter plane for $m = 1.2$, $\alpha = 0.6$ is shown in Fig. 5(a), and for $m = 1.2$, $\alpha = 0.5$ in Fig. 5(b). Fig. 6 presents the 2D bifurcation diagram in the (μ, α)-parameter plane and its enlargement for $m = 1.05$, $B = 1.5$. In these figures different colors correspond to the periodicity regions related to attracting cycles of periods $n \leqslant 30$ (the correspondence of the colors and periods is indicated at the color bar), and white color is related to either higher periodicity regions or to chaotic attractors. Note that several regions of the same color are related to attracting cycles having the same period but different symbolic sequences: for example, in Fig. 6(b) three 5-periodicity regions are clearly visible. As we shown in the next section, the rightmost 5-periodicity region is related to the superstable cycles with symbolic sequences RLM^3 and RLM^2L, the middle region to RL^2ML and RL^2M^2 and the left region to RL^3M and RL^4. The bifurcation curves $BC_{L,1}$, $BC_{L,2}$, BC_R, FB_M as well as the curves BC and BC_J are plotted using their analytical expressions derived in the previous section (note that the boundary $BC_{L,2}$ in Fig. 6 is defined by $\alpha = 0.6$, obtained from $\beta = B\frac{1-\alpha}{\alpha}$ at $\beta = 1$ and $B = 1.5$). Some periodicity regions are additionally marked by the corresponding periods.

As we have already mentioned, two superstable cycles of the map f cannot coexist, while a superstable cycle can coexist with a stable cycle. In Figs. 5 and 6 the regions related to coexisting attractors cannot be seen (except for the narrow green region bounded from above by the subcritical flip bifurcation curve FB_M in Fig. 6(a), related to coexisting attracting fixed point x_M^* and 2-cycle), because only one initial condition has been used to plot these diagrams. The problem of coexistence of different attractors is discussed in the forthcoming paper.

A first observation is related to the particular bifurcation point denoted O in Figs. 5 and 6, which is the intersection point of several border collision curves, namely, $BC_{L,1}$, $BC_{L,2}$ and BC_R. However, it can be clearly seen that not only these bifurcation curves issue from O, but also infinitely many curves bounding periodicity regions which belong to the region *E-II*. Following the notation in [1], the codimension-2 BCB point O is called *organizing center*, defined as a bifurcation point from which an infinite number of bifurcation curves issue.

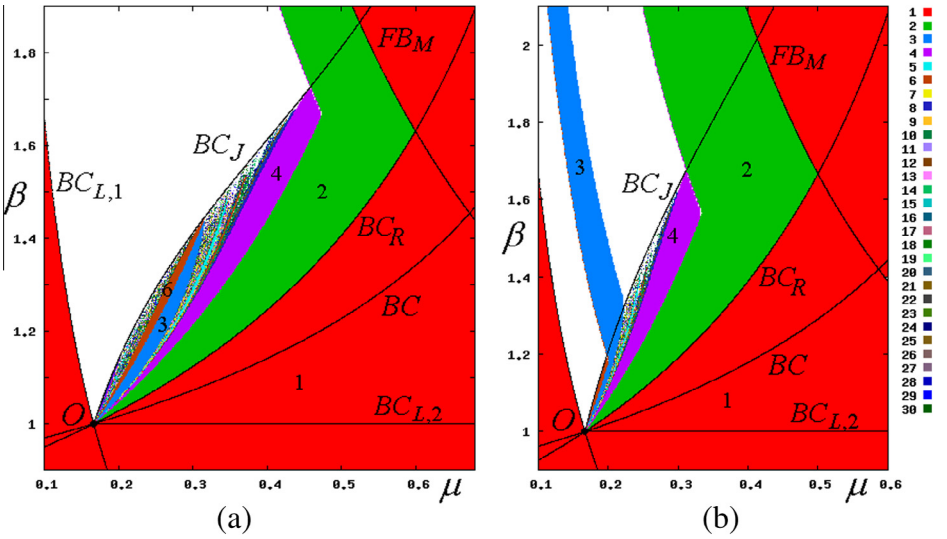

Fig. 5. 2D bifurcation diagram of the map f in the (μ,β)-parameter plane at $m = 1.2$ and $\alpha = 0.6$ in (a), $\alpha = 0.5$ in (b).

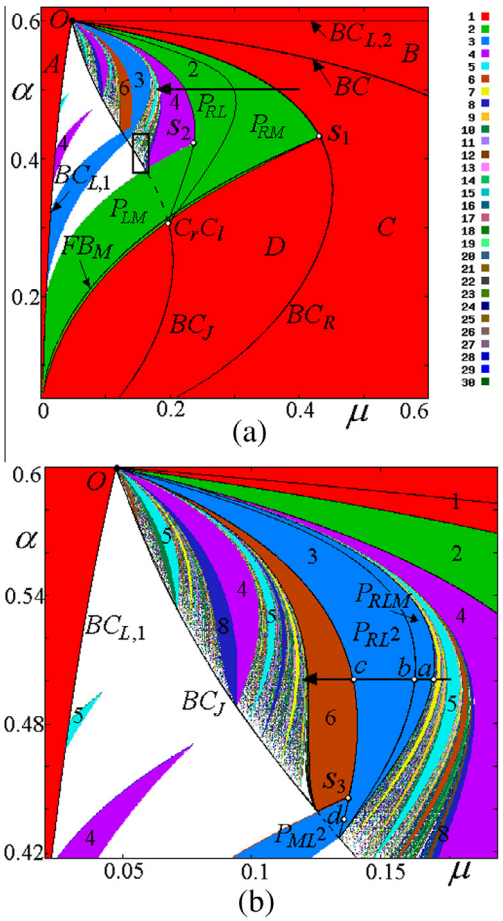

Fig. 6. 2D bifurcation diagram of the map f in the (μ,α)-parameter plane at $m = 1.05$, $B = 1.5$ in (a) and its enlargement in (b). The rectangle marked in (a) is shown enlarged in Fig. 13. (For interpretation of the references to color in this figure legend, the reader is referred to the web version of this article.)

3.1. Boundaries of a periodicity region

Let P_σ denote the periodicity region related to the cycle with the symbolic sequence σ. We first clarify which bifurcations define the boundaries of the regions P_σ using as an example the 3-periodicity region (see Fig. 6(b)). This region consists of three subregions, namely, the regions P_{RLM} and P_{RL^2} related to the superstable 3-cycles with the symbolic sequences RLM and RL^2, respectively, and the region P_{ML^2} related to the stable 3-cycle with the symbolic sequence ML^2. Note that even if a part of the region P_{ML^2} belongs to the region *E-II*, for which the absorbing interval involves all the three branches of f, the stable 3-cycle ML^2 is defined by the functions f_L and f_M only. The region P_{ML} seen in Fig. 6(a) and the region P_{ML^2} seen in Fig. 6(b) belong to both regions *E-I* and *E-II*. For different values of m other periodicity regions, related to stable but not superstable cycles, belonging to *E-I* can extend to *E-II* as well. The boundaries of the regions P_{RL^2} and P_{RLM} shown in Fig. 6(b) are plotted using the conditions of the border collision of the related 3-cycle. Namely, the right boundary of P_{RLM} denoted BC_{C_rLM} is related to the 3-cycle C_rLM as, for example, the cycle shown in Fig. 7(a) (the related parameter point is marked a in Fig. 6(b)); the left boundary BC_{RLC_l} of P_{RLM}, which is also the right boundary of P_{RL^2}, is related to the 3-cycle RLC_l, as, for example, the one shown in Fig. 7(b) (the related parameter point is marked b in Fig. 6(b)) and the left boundary $BC_{C_rL^2}$ of P_{RL^2} corresponds to the 3-cycle C_rL^2, as in Fig. 7(c) (the related parameter point is marked c in Fig. 6(b)). Note that all the three curves BC_{C_rLM}, BC_{RLC_l} and $BC_{C_rL^2}$ issue from the point belonging to the curve BC_J and related to the 3-cycle C_rLC_l.

In a similar way we can obtain the boundaries of the 2-periodicity region shown in green in Fig. 6(a), consisting of three subregions, namely, the regions P_{RM}, P_{RL} and P_{LM}. The lower boundary of P_{RM} (connecting the points marked s_1 and C_lC_r) is related to the 2-cycle C_rM hence denoted as BC_{C_rM}, the right boundary of P_{RM} (connecting s_1 and O) is

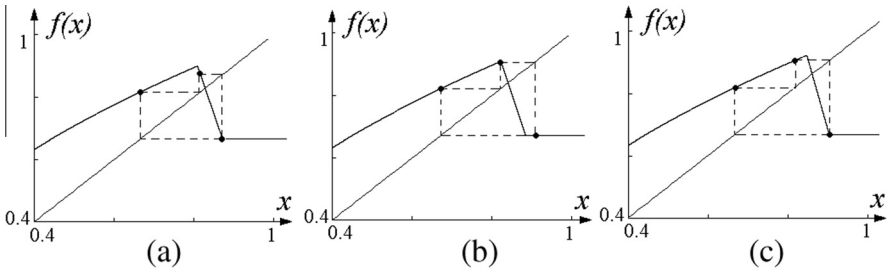

Fig. 7. The 3-cycle γ_3 at the moment of the border collision: in (a) γ_3 has the symbolic sequence C_rLM, in (b) γ_3 is represented by RLC_l and in (c) γ_3 has the symbolic sequence C_rL^2. Here $m = 1.05,\ B = 1.5,\ \alpha = 0.5$ and $\mu = 0.17$ in (a), $\mu = 0.1638$ in (b), $\mu = 0.1394$ in (c) (the related parameter points are marked a, b and c, resp., in Fig. 6(b)).

just the curve BC_R, and its left boundary which is also the right boundary of P_{RL} (connecting C_lC_r and O), corresponds to 2-cycle RC_l, hence denoted as BC_{RC_l}. The left boundary of P_{RL} is related to the cycle C_rL, hence denoted as BC_{C_rL}. The narrow region bounded by the curves BC_{C_rM}, BC_{RC_l} and FB_M (note that $\alpha < 0.5$ here, thus, the flip bifurcation is subcritical) is related to coexisting stable fixed point x^*_M and superstable 2-cycle RM, while the region bounded by BC_{RC_l}, BC_{C_rL} and FB_M is related to the coexistence of the stable fixed point x^*_M and the superstable 2-cycle LR.

This bifurcation structure is schematically illustrated in Fig. 8(a) where the bistability regions mentioned above, as well as the region of coexistence of the stable fixed point x^*_M and the stable 2-cycle LM, are dashed. Additionally it is indicated that stable 2-cycles with symbolic sequences LM^s, RL^s and RM^s (the index s means stability) born due the fold BCB in pair with the unstable cycle MM^u (the index u means that this cycle is unstable) coexist with the stable fixed point x^*_M indicated by the symbol M^s. If the parameter point crosses the curve FB_M the fixed point M^s and the unstable 2-cycle MM^u merge, the fixed point losses stability, the 2-cycle MM^u disappears, so that above the curve FB_M there exist the unstable fixed point x^*_M and the related 2-cycle (stable or superstable). Such a bifurcation structure is observed in the (μ, α)-parameter plane if $\alpha < 0.5$ at the point s_1 and, thus, the flip bifurcation is subcritical (as, for example, it occurs in Fig. 6(a)). The point s_1 is called *border-flip codimension-two bifurcation point*. It is shown in [10] that in general three bifurcation curves are issuing from such a point, among which one is a curve related to the smooth bifurcation and the other two curves are BCB curves.

The bifurcation structure in the case of a supercritical flip bifurcation of x^*_M is schematically illustrated in Fig. 8(b) for $\alpha > 0.5$ at the point C_rC_l. Note that it is possible to have $\alpha < 0.5$ at C_rC_l and $\alpha > 0.5$ at the border-flip point s_1, in which case FB_M intersects with BC_{C_rM}, and it is also possible that the curve FB_M intersects with the curve BC_{C_lM} (for $\alpha > 0.5$ at C_rC_l). In both cases we have $\alpha = 0.5$ at the intersection point, and the flip bifurcation is supercritical above the intersection and subcritical below it.

To see what kind of bifurcation occurs when parameter point crosses boundaries of a periodicity region related to superstable n-cycle, recall first that the only bifurcation which is possible for a superstable cycle, is a BCB. Using the skew tent map as the BCB normal form [34], it is easy to show that a superstable n-cycle γ_n can undergo either a fold BCB, or a flip BCB, or a persistence border collision. In fact, evaluating the left- and right-side derivatives, denoted a and b, of the function f^n at the border-crossing superstable fixed point of f^n at the bifurcation parameter value, we have that one such derivative is obviously 0, say, $a = 0$, and, depending on the other derivative, b, the following cases can be distinguished:

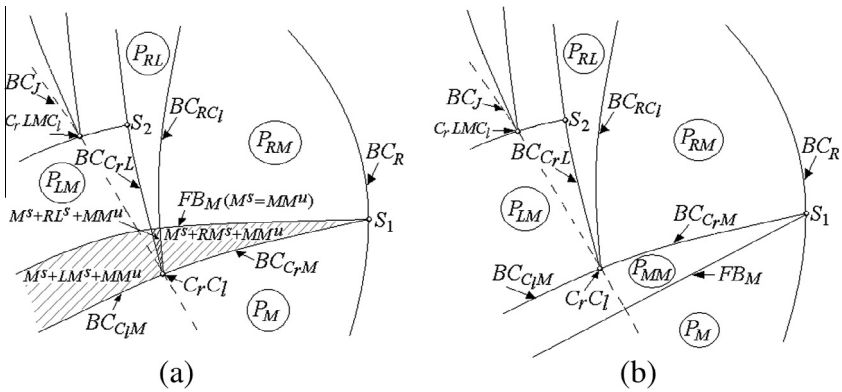

Fig. 8. Schematic structure of the regions P_{RM}, P_{RL} and P_{LM} in the (μ, α)-parameter plane. With $\alpha < 0.5$ at s_1, (a) shows the case of a subcritical flip bifurcation of x^*_M with the bistability regions dashed; with $\alpha > 0.5$ at C_rC_l (b) shows the case of supercritical flip bifurcation of x^*_M.

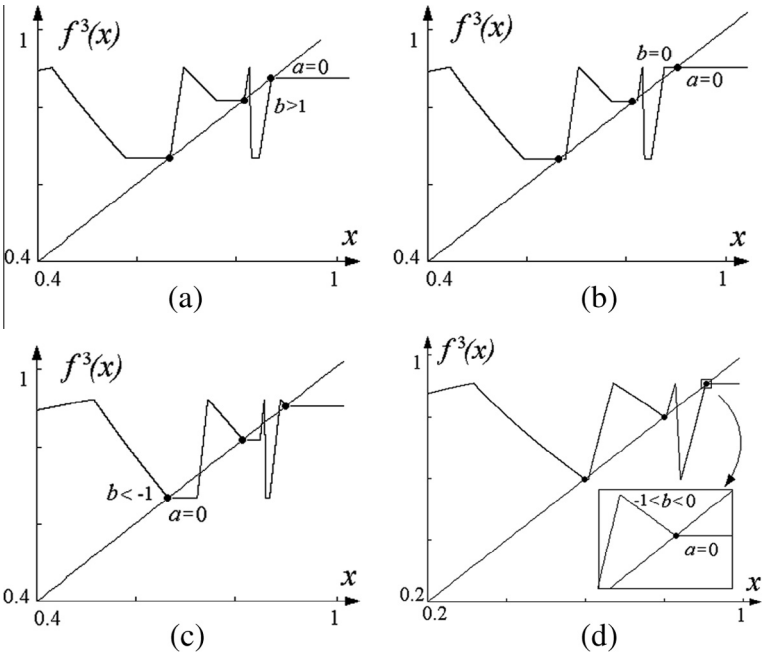

Fig. 9. The map f^3 and its border-crossing fixed points related to the 3-cycle of the map f. Here the parameter values in (a)–(c) are as in Fig. 7, and $\alpha = 0.435$, $\mu = 0.1358$ in (d) (the related parameter points are indicated by a, b, c and d, resp., in Fig. 6(b)).

(1) If $b > 1$ then a *fold BCB* (also referred to as *nonsmooth fold bifurcation*) occurs at which one point of γ_n and one point of the repelling complementary[2] n-cycle collide with the border point simultaneously and both cycles disappear after the bifurcation. An example of f^3 together with the border-crossing fixed points at the moment of the fold BCB is shown in Fig. 9(a); the related parameter point is marked by a in Fig. 6(b).

(2) If $|b| < 1$, then a *persistence border collision* occurs at which the superstable cycle γ_n is transformed into the complementary cycle which is either again superstable, or stable (see Fig. 9(b) and (d), respectively; the related parameter points are marked by b and d in Fig. 6(b)).

(3) If $b < -1$ then a supercritical *flip BCB* occurs at which γ_n is transformed into the complementary repelling n-cycle, while a superstable $2n$-cycle γ_{2n} is born (see Fig. 9(c) and the related parameter point marked by c in Fig. 6(b)).

3.2. Cascades of flip border collision bifurcations

The results of these bifurcations are illustrated in the 1D bifurcation diagram shown in Fig. 10(a), corresponding to the parameter path for fixed $\alpha = 0.5$ varying μ, as indicated in Fig. 6(b) by the horizontal line with an arrow. In particular, it can be seen that at $\mu \approx 0.17$ the boundary BC_{C_rLM} is crossed (see the point a in Fig. 6(b)) and the fold BCB occurs at which for decreasing μ the superstable cycle RLM is born together with the complementary repelling cycle MLM (which is not shown). At the moment of the fold BCB these cycles coincide and have the symbolic sequence C_rLM (see also Fig. 7(a)). At $\mu \approx 0.1638$ the parameter point crosses the boundary BC_{RLC_l} (see the point b in Fig. 6(b)) and the persistence border collision occurs: the cycle RLM is transformed into the cycle RL^2 (the persistence border collision occurs also if the boundary $BC_{C_rL^2}$ is crossed below the point marked by s_3 in Fig. 6(b), e.g., at the point d, in which case we observe the transition from RL^2 to ML^2). At $\mu \approx 0.1394$ the boundary $BC_{C_rL^2}$ is crossed (see the point c in Fig. 6(b)) and the flip BCB occurs leading to the superstable 6-cycle with the symbolic sequence RL^2ML^2.

Fig. 10(b) shows an enlargement of the window indicated in Fig. 10(a), where it can be seen that the superstable 6-cycle RL^2ML^2 for decreasing μ first undergoes the persistence border collision, at $\mu \approx 0.123$, being transformed into the superstable cycle RL^2MLM. Both the sequences RL^2ML^2 and RL^2MLM are the so-called *first harmonics* of RL^2, as explained in the next section. We continue to decrease the value of μ, and at $\mu \approx 0.122$ the flip BCB occurs, leading to the superstable 12-cycle with the symbolic sequence $RL^2MLM^2L^2MLM$. The 12-cycle in its turn also first undergoes the persistence border collision, at $\mu \approx 0.12197$, leading to the cycle $RL^2MLM^2L^2ML^2$ (both $RL^2MLM^2L^2MLM$ and $RL^2MLM^2L^2ML^2$ are the *second harmonics* of RL^2), which then, at $\mu \approx 0.1216$, undergoes the flip BCB resulting to the 24-cycle whose symbolic sequence $RL^2MLM^2L^2ML^2ML^2MLM^2L^2ML^2$ (the *third harmonic* of RL^2). Indeed, an infinite cascade of flip BCBs occurs for decreasing μ which is difficult to observe numerically due to the

[2] Recall that two cycles of a continuous piecewise smooth map, born at a *fold BCB* are so-called *complementary* cycles: their symbolic sequences differ by the one, colliding, symbol.

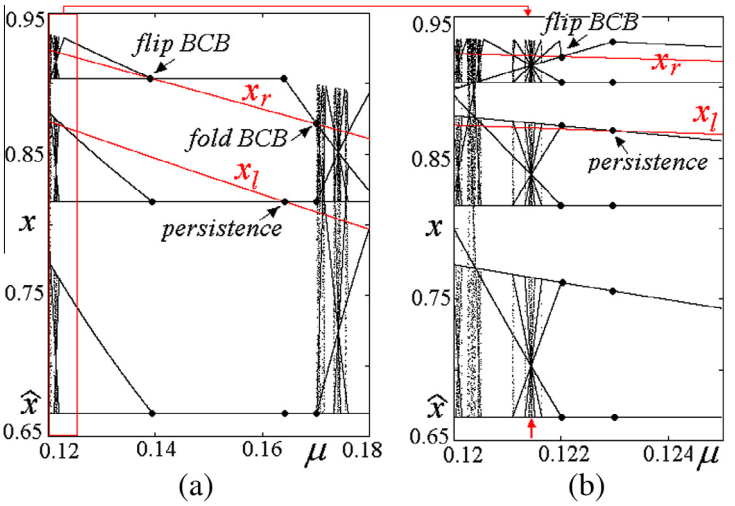

Fig. 10. 1D bifurcation diagram of the map f at $m = 1.05$, $B = 1.5$, $\alpha = 0.5$ and $\mu \in [0.12, 0.18]$ in (a) (the related parameter path is indicated in Fig. 6(b) by the horizontal line with an arrow), and $\mu \in [0.12, 0.125]$ in (b), which is the enlarged window indicated in (a). (For interpretation of the references to color in this figure legend, the reader is referred to the web version of this article.)

high rate of the compression of the related parameter ranges. The sequence of superstable cycles described above can be written schematically as follows:

$$\ldots \xrightarrow{C_r LM} RLM \xrightarrow{RLC_l} RL^2 \xrightarrow{C_r L^2} RL^2ML^2 \xrightarrow{RL^2MLC_l} \tag{22}$$

$$RL^2MLM \xrightarrow{C_r L^2 MLM} RL^2MLM^2L^2MLM \ldots \tag{23}$$

As one more example, let us consider the cascade of flip BCBs of the 2-cycle. It is illustrated in Fig. 11 by means of the 1D bifurcation diagram (the related parameter path for fixed $\alpha = 0.5$ and varying μ is indicated by the horizontal line with an arrow in Fig. 6(a)). Namely, the following sequence of flip BCBs (related to the collision with the border point x_r) and persistence border collisions (due to the collision with the border point x_l) can be observed for decreasing μ. The superstable fixed point x_R^* whose symbolic sequence is just one symbol R, undergoes the flip BCB (the parameter point crosses the boundary BC_R above the point s_1, see Fig. 6(a)), that leads to a 2-cycle with symbolic sequence RM. Then this cycle is transformed into the one with symbolic sequence RL due to the persistence border collision (the parameter point crosses the boundary BC_{RC_L}). Note that the sequences RM and RL are the first harmonics of R. Then the 2-cycle RL undergoes the flip BCB (the parameter point crosses the boundary BC_{C_rL} above the point s_2) leading to a 2^2-cycle whose symbolic sequence is $RLML$. Then this cycle changes its symbolic sequence to RLM^2 due to persistence border collision ($RLML$ and RLM^2 are the second harmonics of R). Then it undergoes the flip BCB leading to a 2^3-cycle with the symbolic sequence RLM^3LM^2 which is transformed into RLM^3LML

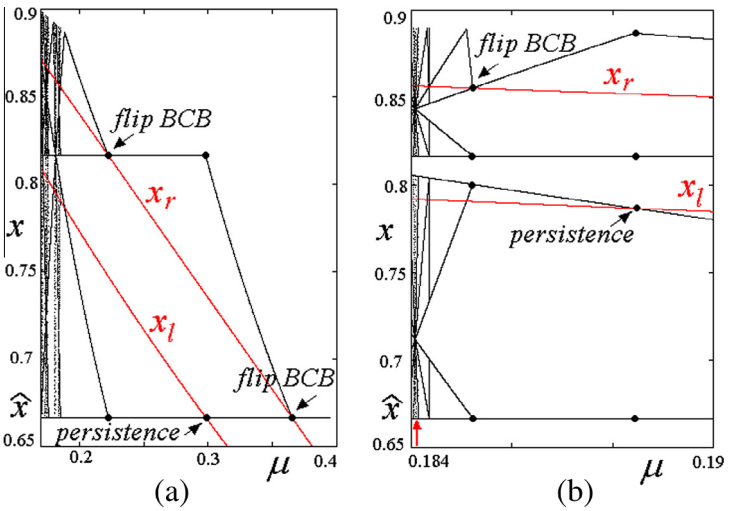

Fig. 11. 1D bifurcation diagram of the map f at $m = 1.05$, $B = 1.5$, $\alpha = 0.5$, and $\mu \in [0.175, 0.4]$ in (a) (the related parameter path is indicated in Fig. 6(a) by the horizontal line with an arrow); $\mu \in [0.184, 0.19]$ in (b) (it is an enlargement of (a)).

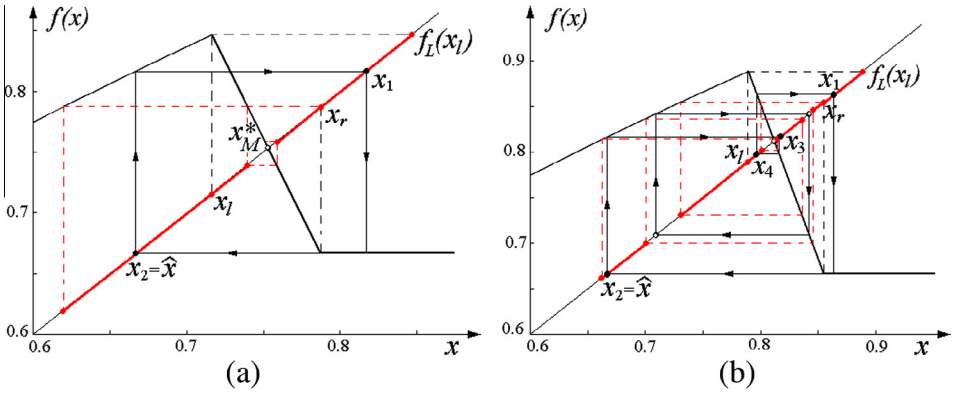

Fig. 12. In (a) the cycle $\gamma_2 = \{x_i\}_{i=1}^2$ and in (b) the cycle $\gamma_4 = \{x_i\}_{i=1}^4$ which is the first harmonic of γ_2, are shown. Any point of $J = [\hat{x}, f(x_l)]$ is mapped into the attractor except for x^*_M in (a), and except for x^*_M, the 2-cycle LM (shown by white circles) and its preimages in (b). Here $m = 1.05$, $B = 1.5$, $\alpha = 0.5$ and $\mu = 0.25$ in (a), $\mu = 0.186$ in (b).

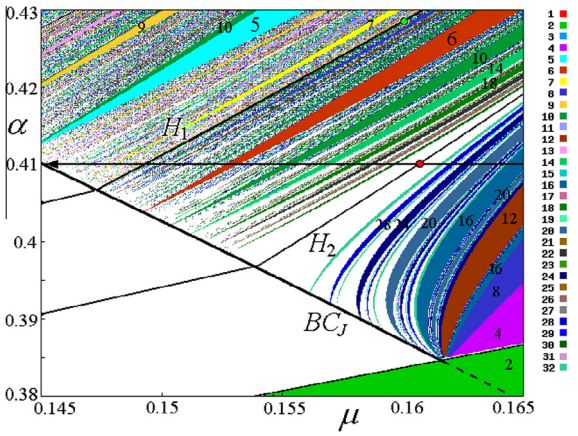

Fig. 13. An enlargement of the window indicated in Fig. 6(a) by the rectangle. The curves marked H_1 and H_2 are related to the first homoclinic bifurcations of the fixed point x^*_M and 2-cycle with the symbolic sequence LM, respectively. (For interpretation of the references to color in this figure legend, the reader is referred to the web version of this article.)

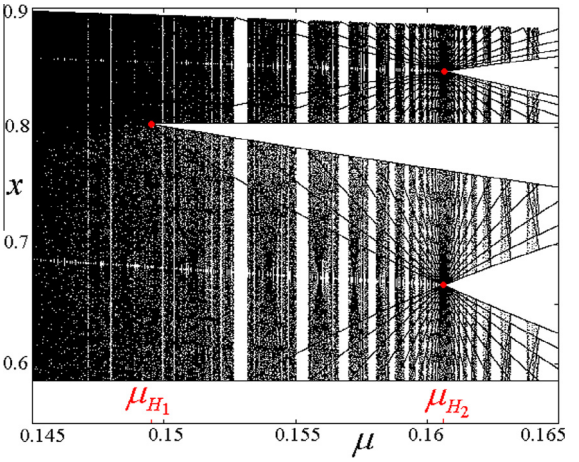

Fig. 14. 1D bifurcation diagram of the map f at $m = 1.05$, $B = 1.5$, $\alpha = 0.41$ and $\mu \in [0.145, 0.165]$ (the related parameter path is indicated in Fig. 13 by the horizontal line with an arrow). The values $\mu = \mu_{H_1}$ and $\mu = \mu_{H_2}$ correspond to the first homoclinic bifurcations of the fixed point and 2-cycle, respectively.

due to the persistence border collision (RLM^3LM^2 and RLM^3LML are the third harmonics of R), so on, that can be schematically represented as follows:

$$R \xrightarrow{C_r} RM \xrightarrow{RC_l} RL \xrightarrow{C_rL} RLML \xrightarrow{RLMC_l} RLM^2 \xrightarrow{C_rLM^2} RLM^3LM^2 \ldots \quad (24)$$

As we have mentioned in the previous section, in the case of the superstable 2-cycle RL or any of its harmonics, the basin of attraction defined in (21) has a simpler structure than in the generic case, being not associated with a chaotic repeller on the basin boundary. For example, it is easy to see that in case of the 2-cycle RL shown in Fig. 12(a), any point of the absorbing interval $J = [\hat{x}, f(x_l)]$, except for the unstable fixed point x^*_M, is mapped into this cycle in a finite number of iterations while in case of the 4-cycle RLM^2 shown in Fig. 12(b), any point of J is mapped into this cycle except for the unstable fixed point x^*_M, unstable 2-cycle LM and its preimages (converging in backward iterations by f_M^{-1} to x^*_M). In general, for a superstable cycle whose symbolic sequence is the kth harmonic of R, $k > 0$, the basin boundary includes the fixed point x^*_M, the points of all the m-harmonic cycles for any $m < k$ (which are unstable due to flip BCBs), as well as their preimages. Such a structure of the basin boundary is qualitatively similar to the one of an attracting 2^k-cycle of the logistic map born during the first cascade of period-doubling bifurcations.

3.3. Homoclinic bifurcations and Milnor attractors

Let us now consider the sets in the parameter space to which the periodicity regions of the superstable cycles are accumulating, and the dynamics related to these sets. Such accumulation parameter values are visible in the 1D bifurcation diagrams as those related to the "bodies of the spiders", like, for example, the value $\mu = 0.1215$ indicated by a red arrow in Fig. 10(b). For the logistic map it

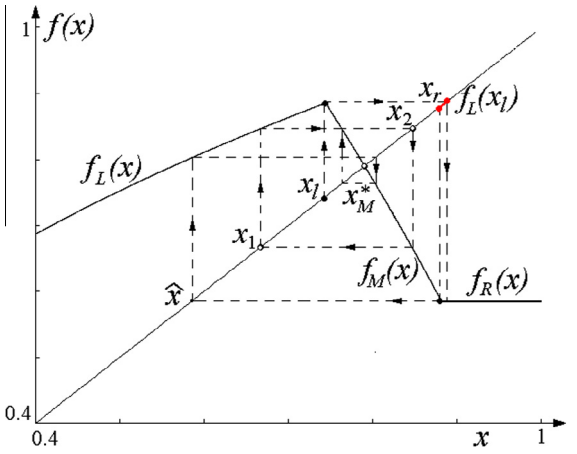

Fig. 15. The map f for the parameter values corresponding to the first homoclinic bifurcation of the 2-cycle $\gamma_2 = \{x_1, x_2\}$. Here $m = 1.05$, $B = 1.5$, $\alpha = 0.41$ and $\mu = 0.160635 \approx \mu_{H_2}$. The related parameter point belongs to the curve H_2 and is marked by the red circle in Fig. 13. (For interpretation of the references to color in this figure legend, the reader is referred to the web version of this article.)

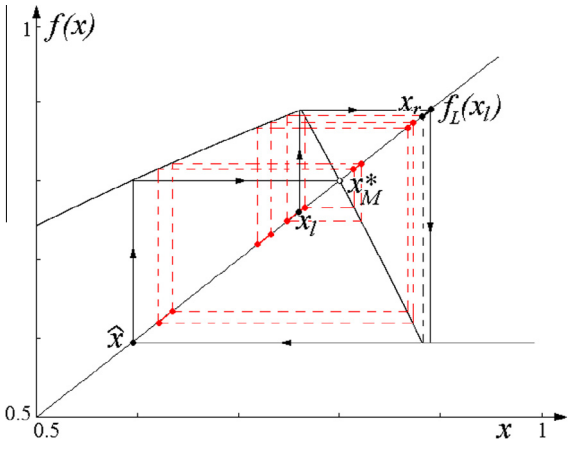

Fig. 16. The map f for the parameter values related to the first homoclinic bifurcation of the fixed point M. Here $m = 1.05$, $B = 1.5$, $\mu = 0.16$, $\alpha = 0.4285$. This parameter point belongs to the curve H_1 and marked by the green circle in Fig. 13. (For interpretation of the references to color in this figure legend, the reader is referred to the web version of this article.)

is known that the periodicity windows at the well-known 1D bifurcation diagram are accumulating to the parameter values related to homoclinic bifurcations of the unstable cycles. Moreover, on the other side of any accumulation point of a cascade of period-doubling bifurcations, a cascade of the homoclinic bifurcations is accumulating. To see that for the map f the periodicity regions are accumulating on the parameter sets related to homoclinic bifurcations of the corresponding cycles, we first present in Fig. 13 the enlargement of the window marked by the rectangle in Fig. 6(a), and in Fig. 14 the 1D bifurcation diagram related to the parameter path indicated in Fig. 13 by the horizontal line with an arrow which pierces the red circle on the line H_2. In this diagram the accumulation points $\mu = \mu_{H_1}$ and $\mu = \mu_{H_2}$ are clearly visible, related to the first homoclinic bifurcations of the fixed point x^*_M and of the 2-cycle with the symbolic sequence LM, respectively.

Let us first consider the 2-cycle with the symbolic sequence LM, that is, the cycle $\gamma_2 = \{x_1, x_2\}$ where $x_1 < x_l$, $x_l < x_2 < x_r$, $f_L(x_1) = x_2$ and $f_M(x_2) = x_1$. Its first homoclinic bifurcation is defined by the condition of the border point x_l to be preperiodic to this cycle, namely, as illustrated in Fig. 15, this condition can be written as

$$f_M \circ f_M \circ f_L \circ f_R \circ f_L(x_l) = x_2 \tag{25}$$

or, taking into account that for the parameter region *E-II* we have $f_R \circ f_L(x_l) = f_R(x_r)$, the condition in (25) becomes

$$f_M \circ f_M \circ f_L \circ f_R(x_r) = x_2$$

and from $f_R(x) = \hat{x}$ we have:

$$f_M \circ f_M \circ f_L(\hat{x}) = x_2. \tag{26}$$

The bifurcation curve numerically obtained corresponding to the condition in (26) is denoted H_2 in Fig. 13. In Fig. 15 we present the map f at the moment of the first homoclinic bifurcation of the 2-cycle (the related point of the curve H_2 is marked by red circle in Fig. 13). It can be seen that even if this cycle is locally repelling, almost all the points of the absorbing interval $J = [\hat{x}, f(x_l)]$ are mapped into this cycle, so it is an attractor in Milnor sense.[3] In the considered map such an attractor occurs due to the flat branch $f_R(x)$, namely, the complete interval $[x_r, \infty)$ is ultimately mapped to the point x_2, as well as infinitely many preimages of the interval $[x_r, f_L(x_l)]$ marked by red in Fig. 15. Its preimages of increasing rank fill densely the interval J and define the stable set, given in (21), of the locally repelling 2-cycle γ_2. We notice that any homoclinic cycle of the map f for the considered parameter range has the stable set as given in (21). Clearly in J there exist also infinitely many points which are not attracted to the cycle γ_2, which belong to the chaotic repeller of zero Lebesgue measure consisting of the points of all the repelling cycles, their preimages of any rank and their limit sets.

One more example is shown in Fig. 16 where the function f is plotted at the parameter values corresponding to the first homoclinic bifurcation of the fixed point x^*_M (the related parameter point belongs to the curve H_1 and marked by green circle in Fig. 13), which in our case also leads to an attractor in Milnor sense, whose stable set is as given in (21). A few preimages of the interval $[x_r, f_L(x_l)]$ are shown in red in Fig. 16, and all the existing preimages are filling densely the interval J. The condition of the first homoclinic bifurcation of x^*_M is given by

$$f_L \circ f_R(x_r) = x^*_M, \tag{27}$$

where the fixed point x^*_M is implicitly defined from $x^*_M = f_M(x^*_M)$. The bifurcation curve related to the condition in (27) is denoted H_1 in Fig. 13.

[3] Recall that a *Milnor attractor* [28] is defined as a closed invariant set $A \subset J$ such that the set $\rho(A)$ consisting all the points $x \in J$ for which $\omega(x) \subset A$ has *strictly positive* measure, and $\rho(A')$ coincides with $\rho(A)$ up to a set of measure zero. Here $\omega(x)$ is the set of accumulation points of the orbit under the forward iterations of x, called ω-limit set of x.

4. Modified U-sequence

The numerical results presented in the previous section suggest that the periodicity regions of the superstable cycles of the map f given in (8) are ordered according to the well-known U-sequence. Recall that the U-sequence (where "U" stands for "universal") was first described in [27] and referred to symbolic sequences of *superstable* cycles of maps of a particular class. Namely, it was established for 1D continuous piecewise differentiable maps $g: I \to I$ depending on a parameter, with a unique maximum g_{max} assumed either at a point or in an interval, and such that to the left or right of this point (or interval) the map is strictly increasing or strictly decreasing, respectively. Additionally it was assumed that at any x such that $g(x) = g_{max}$ the derivative of g exists and is equal to 0, and the condition defining the parameter range. The most known example of maps whose superstable cycles are ordered on parameter according to the U-sequence are unimodal maps with "smooth" maximum, in which case the U-sequence can be easily extended to the sequence of *stable* cycles, as we clarify below using the logistic map as an example (recall that a 1D continuous map $g: I \to I$ is called *unimodal* if there exists exactly one point of local extrema in the interior of I, moreover, g is strictly increasing on one side of the point of local extrema and strictly decreasing on the other side). However, in [27] it was also mentioned, that the conditions listed above are sufficient to guarantee the existence of the U-sequence, but not necessary. In fact, it is known (see, e.g., [17]) that the U-sequence is valid also for the unimodal maps which are not differentiable at the point of maximum (as, for example, the considered map f for parameter values belonging to the region *E-I* given in (18), or the skew tent map), in which case the U-sequence may be related to not only stable but also *unstable* cycles, or even unstable cycles only (in [27] the U-sequence in the tent map was mentioned as an example of such a case). Obviously, the considered map f for parameter values belonging to the region *E-II* given in (19) does not belong to the classes of maps mentioned above. To see why the U-sequence is nevertheless valid for our map, let us consider the map $g: I \to I$ defined as follows:

$$g: x \mapsto g(x) = \begin{cases} f_L(x) = x^{\alpha} & \text{for } 0 < x \leqslant x_a, \\ f_C(x) = x_c^{\alpha} & \text{for } x_a < x \leqslant x_c, \\ f_M(x) = \left[\frac{1}{\mu\beta}\left(1 - \frac{x}{m}\right)\right]^{\frac{\alpha}{1-\alpha}} & \text{for } x_c < x \leqslant x_r, \\ f_R(x) = \widehat{x} & \text{for } x > x_r, \end{cases} \tag{28}$$

where $x_a = f_L^{-1}(x_r)$, $x_c = f_M^{-1}(x_r)$, $\widehat{x} = \left(\frac{1}{\beta}\right)^{\frac{\alpha}{1-\alpha}}$, $x_r = m(1-\mu)$, and parameters α, β, μ and m satisfy (2) and (19) (see an example of the map g in Fig. 17). The map g is constructed from the map f by introducing a new flat branch $f_C(x)$ defined on the interval bounded by two preimages of the border point x_r, so that the absorbing interval of g is $J = [\widehat{x}, x_r]$ and the flat branch $f_R(x)$ plays no role for the dynamics. Clearly, the map g belongs to the class of maps considered in [27] (see also [9]), thus, the U-sequence is valid for such a map (of course, to discuss the U-sequence in the map g we need to specify the related parameter path). On the other hand, it is easy to see that the map g is topologically conjugate to the considered map f, thus, the U-sequence is valid for it as well.

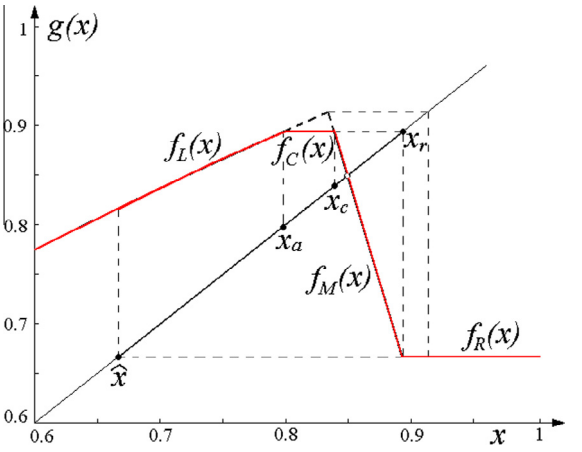

Fig. 17. The map g defined in (28) at $m = 1.05$, $B = 1.5$, $\alpha = 0.5$ and $\mu = 0.15$.

Before we describe the U-sequence of the map f let us recall in short how the standard U-sequence is formed using the logistic map $g: x \mapsto g(x) = ax(1-x)$, $3 < a < 4$, as an example. In [27] the U-sequence is constructed for the superstable cycles, for which the first letter in the symbolic sequence is C (corresponding to the point of maximum, separating the two partitions, L and R), and it is omitted. For example, the symbolic sequence of the superstable 3-cycle is $RL \equiv CRL$. Note that due to the fold bifurcation two 3-cycles are born, stable and unstable, with the same symbolic sequence, namely, RRL. Then, increasing a, at a suitable value the stable cycle becomes superstable, that is, it has the symbolic sequence CRL, and after we have the stable cycle with LRL sequence (which soon after becomes unstable via the flip bifurcation) while the unstable cycle, born in pair with the stable one, always persists with the sequence RRL. We can say that the sequence RL of the superstable 3-cycle *represents both the* 3*-cycles*, with the sequences LRL and RRL. As a different example consider the sequence $RLR \equiv CRLR$ of the superstable 4-cycle. It *represents only one cycle*, namely, the 4-cycle with the symbolic sequence $RRLR$. Indeed, the sequence RLR is the first harmonic of R which represents the cycle born due to the period-doubling bifurcation of the 2-cycle. Recall that the (first) harmonic of a symbolic sequence σ is the sequence $\sigma\kappa\sigma$, where $\kappa = L$ if the number of R in σ is odd while $\kappa = R$ if this number is even. The k-harmonic is constructed by k consecutive applications of the same rule.

If we consider all the symbolic sequences of the logistic map related to its superstable cycles up to some period m, then these symbolic sequences belong to the U-sequence (the complete U-sequence includes all the admissible symbolic sequences of the superstable cycles of a unimodal map), and they are ordered for increasing values of the parameter a according to the following rule. For two different symbols $\kappa \neq \nu$, the order of κ and ν is in the sense of the natural order: $L < C < R$. Given two symbolic sequences $\sigma_1 = \sigma\kappa$ and $\sigma_2 = \sigma\nu$ with common string σ

and next symbol $\kappa \neq \nu$, the order of σ_1 and σ_2 is the same (opposite) as the order of κ and ν if the number of R in σ is even (odd). For example, comparing two symbolic sequences of the superstable 4-cycles, $\sigma_1 = RL^2$ and $\sigma_2 = RLR$, we see that the number of R in their common string $\sigma = RL$ is odd, while the next symbols are L in σ_1 and R in σ_2, and $L < R$. Thus, we have that $RL^2 > RLR$.

The rule described above implies, in particular, that the symbolic sequence of the so-called basic n-cycle is the largest among the symbolic sequences of the other n-cycles.[4] Recall that a basic n-cycle has only one symbol R in its symbolic sequence, that is, this sequence is RL^{n-2}. It can also be shown [27] that the k- and $(k+1)$-harmonics of some symbolic sequence for any integer $k > 0$ are adjacent in the U-sequence (i.e., there are no any other symbolic sequences in between them). For example, the order of the symbolic sequences of the cycles of period $2 \leqslant n \leqslant 6$ of a unimodal map is the following:

$$R < RLR < RLR^3 < RLR^2 < RL < RL^2RL < RL^2R < RL^2R^2 < RL^2 < RL^3R < RL^3 < RL^4, \quad (29)$$

where the first or, equivalently, the last symbol, is C (which is omitted). Note that other symbolic sequences of higher periods exist between any two consecutive sequences but not between a sequence and its harmonic.

Let us now turn to the U-sequence observed in the map f. As we have already mentioned, we need first to specify an appropriate parameter path, which, roughly speaking, has to cross all the existing periodicity regions. Consider first the region E-I. As an appropriate parameter path in the (μ, β)-parameter plane (for values of α and m fixed as, for example, in the case shown in Fig. 5) we can consider a cross-section of E-I from the right boundary FB_M to the left boundary $BC_{L,1}$. In the (μ, α)-parameter plane (for the values of B and m fixed as, for example, in the case shown in Fig. 6) an appropriate parameter path can be the one connecting a point of the boundary FB_M with the organizing center O. Given that the map f for parameter values belonging to the region E-I is unimodal (and its cycles have symbolic sequences consisting of symbols L and M only), the order (29) is valid for f as well: we simply have to substitute the symbol R by M, while the first (omitted) symbol C corresponds to the symbol C_l:

$$M < MLM < MLM^3 < MLM^2 < ML < ML^2ML < ML^2M < ML^2M^2 < ML^2 < ML^3M < ML^3 < ML^4. \quad (30)$$

It is worth to emphasize that differently from the logistic map, the sequence given above is not related to the superstable cycles, but to the cycles one point of which is x_l (where f is not differentiable).

Now we adjust the standard U-sequence to describe the cycles which can be observed in the map f when the parameters belong to the region E-II. An appropriate parameter path has to cross all the periodicity regions of superstable cycles. For example, we can vary the parameter values along an arc connecting the point marked by s_1 in Fig. 6a with the organizing center O. In each of the symbolic sequences constituting the order (30), the first symbol M corresponding to the maximal periodic point, has to be substituted by R (and, as we have already noticed, only one point R can exist in a symbolic sequence):

$$R < RLM < RLM^3 < RLM^2 < RL < RL^2ML < RL^2M < RL^2M^2 < RL^2 < RL^3M < RL^3 < RL^4. \quad (31)$$

Such a sequence corresponds to the order of the superstable cycles of f one point of which is x_l, with the symbol C_l omitted in the above order. The generic rule recalled above to determine the order of such sequences, has to be modified taking into account that one letter R takes the place of one letter M in the standard U-sequence. So, the rule for the order (31) is as follows. Given two different symbols $\kappa \neq \nu$, the order of κ and ν is, as before, in the sense of the natural order: $L < C_l < M$. Given two symbolic sequences $\sigma_1 = \sigma\kappa$ and $\sigma_2 = \sigma\nu$ with common string σ and next symbol $\kappa \neq \nu$, the order of σ_1 and σ_2 is the same (opposite) as the order of κ and ν if the number of M in σ is odd (even).

Let us now extend the order (31) to all the superstable cycles of the map f (i.e., not only those with periodic point x_l). As we have seen, the curves corresponding to the cycles with point x_l are related to the persistence border collisions and located inside the periodicity regions of the corresponding superstable cycles. In some sense, these curves constitute a skeleton of the overall "superstable" bifurcation structure, quite similar to the parameter values of the superstable cycles of the logistic map, located inside the related periodicity windows. To construct the complete sequence we can substitute each symbolic sequence σ by two new sequences, σL and σM, ordered according to the rule stated above. For example, the sequence R related to the superstable 2-cycle RC_l can be substituted by two sequences, RM and RL (representing the related superstable 2-cycles) ordered as $RM < RL$. The sequence RLM representing superstable 4-cycle $RLMC_l$ can be substituted by $RLML$ and $RLMM$ ordered as $RLML < RLMM$ (cf. with (24)). One more example is the sequence $RL \equiv RLC_l$ representing the superstable 3-cycle which can be substituted by $RLM < RLL$.

Thus, the complete order of the superstable cycles periods $2 \leqslant n \leqslant 6$ of the map f is the following:

$$RM < RL < RLML < RLM^2 < RLM^3L < RLM^4 < RLM^3 < RLM^2L < RLM < RL^2 < RL^2ML^2 < RL^2MLM < RL^2ML < RL^2M^2 < RL^2M^3 < RL^2M^2L < RL^2M < RL^3 < RL^3ML < RL^3M^2 < RL^3M < RL^4 < RL^4M < RL^5. \quad (32)$$

5. Conclusions

To summarize, we have obtained an analogue of the U-sequence according to which the periodicity regions related to the superstable cycles of the map f defined in (8) are ordered. As an economic interpretation of the obtained results we note that in the credit cycle model defined by the map f, the economy experiences a fluctuation of the

[4] For a prime period $n > 2$ the number of stable n-cycles having different symbolic sequences is $k(n) = (2^{n-1} - 1)/n$. For the case in which n is nonprime see, e.g., [17].

entrepreneur net worth due to changing composition of the credit between the two types of projects, the Good and the Bad. When the current net worth is very low, the entrepreneurs cannot finance the Bad projects, because the borrowing constraint is too tight. All credit thus goes to the Good projects, and hence, a higher current net worth leads to a higher net worth in the next period. When the current net worth is in the intermediate range, the Bad projects are financed but still subject to the borrowing constraint, so that a higher current net worth, by making the Bad projects more appealing, reduces the credit flow to the Good, which causes a decline in the net worth in the next period. When the current net worth is very high, the Bad projects are no longer subject to the borrowing constraint, so that a higher current net worth would not make the Bad projects more appealing, so that the credit flow to the Good, and hence the net worth in the next period, is not affected. We have studied the bifurcation structure of the region *E-II* given in (19), related to the superstable cycles generated by this model, in the terms of the parameters representing the share of capital in the Cobb–Douglas production function, the profitability of the Bad project, as well as the pledgeability of the revenues of the Bad projects and the fixed investment requirement of the Bad projects, which jointly affect the tightness of their borrowing constraint. It is important to emphasize that superstable cycles created due to the constant branch of the map f are persistent under parameter perturbations. The bifurcation structure in the parameter region *E-I* given in (18) which, differently from *E-II*, includes regions related to chaotic attractors, as well as the periodicity regions belonging to *E-II* but not related to the superstable cycles, is discussed in a forthcoming paper.

Acknowledgments

This work has been performed within the activity of the project PRIN 2009 "Local interactions and global dynamics in economics and finance: models and tools", MIUR, Italy, and under the auspices of COST Action IS1104 "The EU in the new complex geography of economic systems: models, tools and policy evaluation".

References

[1] Avrutin V, Schanz M. Multi-parametric bifurcations in a scalar piecewise-linear map. Nonlinearity 2006;19:531–52.
[2] Avrutin V, Futter B, Schanz M. The discontinuous top tent map and the nested period incrementing bifurcation structure. Chaos Solitons Fractals 2012;45:465–82.
[3] Avrutin V, Futter B, Gardini L, Schanz M. Unstable orbits and Milnor attractors in the discontinuous flat top tent map. ESAIM (Eur Ser Appl Ind Math) 2012;36:126–58.
[4] Banerjee S, Karthik MS, Yuan G, Yorke JA. Bifurcations in one-dimensional piecewise smooth maps-theory and applications in switching circuits. IEEE Trans Circuits Syst-I Fundam Theory Appl 2000;47:389–94.
[5] Banerjee S, Verghese GC, editors. Nonlinear phenomena in power electronics: attractors, bifurcations, chaos, and nonlinear control. New York: IEEE Press; 2001.
[6] Bischi GI, Chiarella C, Kopel M, Szidarovszky F. Nonlinear oligopolies: stability and bifurcations. Heidelberg: Springer; 2009.
[7] Brianzoni S, Michetti E, Sushko I. Border collision bifurcations of superstable cycles in a one-dimensional piecewise smooth map. Math Comput Simul 2010;81(1):52–61.
[8] Brogliato B. Nonsmooth mechanics – models, dynamics and control. New York: Springer-Verlag; 1999.
[9] Brucks KM, Misiurewicz M, Tresser C. Monotonicity properties of the family of trapezoidal maps. Commun Math Phys 1991;137:1–12.
[10] Colombo A, Dercole F. Discontinuity induced bifurcations of nonhyperbolic cycles in nonsmooth systems. SIAM J Imaging Sci 2010;3(1):62–83.
[11] Dankowicz H, Nordmark AB. On the origin and bifurcations of stick–slip oscillations. Physica D 2000;136(3–4):280–302.
[12] Day R. Complex economic dynamics. Cambridge: MIT Press; 1994.
[13] di Bernardo M, Feigin MI, Hogan SJ, Homer ME. Local analysis of C-bifurcations in *n*-dimensional piecewise smooth dynamical systems. Chaos Solitons Fractals 1999;10:1881–908.
[14] di Bernardo M, Budd CJ, Champneys AR, Kowalczyk P. Piecewise-smooth dynamical systems: theory and applications, applied mathematical sciences, vol. 163. London: Springer-Verlag; 2007.
[15] Feigin MI. Doubling of the oscillation period with C-bifurcations in piecewise-continuous systems. Prikl Math Mekh 1970;34:861–9.
[16] Gardini L, Sushko I, Naimzada A. Growing through chaotic intervals. J Econ Theory 2008;143:541–57.
[17] Hao BL. Elementary symbolic dynamics and chaos in dissipative systems. Singapore: World Scientific; 1989.
[18] Hommes C, Nusse H. Period three to period two bifurcation for piecewise linear models. J Econ 1991;54(2):157–69.
[19] Huang W, Day R. Chaotically switching bear and bull markets: the derivation of stock price distributions from behavioral rules. In: Day R, Chen P, editors. Nonlinear dynamics and evolutionary economics. Oxford: Oxford University Press; 1993. p. 169–82.
[20] Ito S, Tanaka S, Nakada H. On unimodal transformations and chaos II. Tokyo J Math 1979;2:241–59.
[21] Maistrenko YL, Maistrenko VL, Chua LO. Cycles of chaotic intervals in a time-delayed Chua's circuit. Int J Bifurcation Chaos 1993;3:1557–72.
[22] Matsuyama K. Good and bad investment: an inquiry into the causes of credit cycles. Center for Mathematical Studies in Economics and Management, Science Discussion Paper No. 1335, Northwestern University; 2001.
[23] Matsuyama K. Credit traps and credit cycles. Am Econ Rev 2007;97:503–16.
[24] Matsuyama K. The good, the bad, and the ugly: an inquiry into the causes and nature of credit cycles. Theor Econ 2013;8:623–51.
[25] Matsuyama K, Sushko I, Gardini L. Chaos in a model of credit cycles with good and bad projects. Presented at the eighth international conference of nonlinear economic dynamics, Richard Goodwin Centennial, Siena, Italy; July 2013 (Downloadable from <http://faculty.wcas.northwestern.edu/~kmatsu/>).
[26] Leonov NN. Map of the line onto itself. Radiofisika 1959;3(3):942–56.
[27] Metropolis N, Stein ML, Stein PR. On finite limit sets for transformations on the unit interval. J Comb Theory 1973;15:25–44.
[28] Milnor J. On the concept of attractor. Commun Math Phys 1985;99:177–95.
[29] Nordmark AB. Universal limit mapping in grazing bifurcations. Phys Rev E 1997;55:266–70.
[30] Nusse HE, Yorke JA. Border-collision bifurcations including period two to period three for piecewise smooth systems. Physica D 1992;57:39–57.
[31] Nusse HE, Yorke JA. Border-collision bifurcation for piecewise smooth one-dimensional maps. Int J Bifurcation Chaos 1995;5:189–207.
[32] Puu T, Sushko I, editors. Oligopoly dynamics, models and tools. New York: Springer-Verlag; 2002.
[33] Sushko I, Agliari A, Gardini L. Bifurcation structure of parameter plane for a family of unimodal piecewise smooth maps: border-collision bifurcation curves. In: Bischi GI, Sushko I, editors. Dynamic modeling in economics and finance in honor of Professor Carl Chiarella. Chaos, Solitons & Fractals, vol. 29 (3). p. 756–70.
[34] Sushko I, Gardini L. Degenerate bifurcations and border collisions in piecewise smooth 1D and 2D maps. Int J Bifurcation Chaos 2010;20:2045–70.
[35] Tramontana F, Gardini L, Westerhoff F. Heterogeneous speculators and asset price dynamics: further results from a one-dimensional discontinuous piecewise-linear model. Comput Econ 2011;38:329–47.
[36] Zhusubaliyev ZT, Mosekilde E. Bifurcations and chaos in piecewise-smooth dynamical systems. Singapore: World Scientific; 2003.
[37] Zhusubaliyev ZT, Mosekilde E, Maity S, Mohanan S, Banerjee S. Border collision route to quasiperiodicity: numerical investigation and experimental confirmation. Chaos 2006;16:1–11.